
ESTIMATING EXCESS COVID-19 INFECTIONS WITH NONPARAMETRIC SELF-EXCITING POINT PROCESSES

A PREPRINT

Peter Boyd
Department of Statistics
Oregon State University
Corvallis, Oregon
boydpe@oregonstate.edu

James Molyneux
Department of Statistics
Oregon State University
Corvallis, Oregon
molyneuj@oregonstate.edu

April 29, 2022

Abstract

The COVID-19 pandemic has led to a vast amount of growth for statistical models and methods which characterize features of disease outbreaks. One class of models that came to light in this regard has been the use of self-exciting point processes, wherein infections occur both “at random” and also more systematically from person-to-person transmission. Beyond the modeling of the overall COVID-19 outbreak, the pandemic has also motivated research assessing various policy decisions and event outcomes. One such area of study, addressed here, relates to the formulation of methods which measure the impact that large events or gatherings of people had in the local areas where the events were held. We formulate an alternative approach to traditional causal inference methods and then apply our method to assessing the impact that then President Donald Trump’s re-election campaign rallies had on COVID-19 infections in areas where the rallies were hosted. By incorporating several adaptations to nonparametric self-exciting point process models, we estimate both the excess number of COVID-19 infections brought on by the rallies and the duration of time in which these excess infections persisted.

Keywords Causal inference · Disease modeling · Public health · Epidemiology

1 Introduction

The global COVID-19 pandemic has resulted in an explosion of research surrounding the statistical modeling of epidemics (see for example [Malloy et al., 2021], [Bonalumi et al., 2020]). The pandemic has also yielded research related to how events ([Dave et al., 2021], [Hadianfar et al., 2021]) or government policies ([Wang, 2021], [Cho, 2020]) have impacted various aspects of the outbreak, such as infection and hospitalization rates, case fatality rates, etc.

Self-exciting point processes are one class of models that have seen increased use in the spatio-temporal modeling and forecasting of the COVID-19 pandemic [Bertozzi et al., 2020, Browning et al., 2021]. Initially developed by [Hawkes, 1971], this model class has been utilized extensively in the study of earthquakes ([Ogata, 1988], [Ogata, 1998]) and has also been applied to areas such as wildfires [Peng et al., 2005], invasive species [Balderama et al., 2012], mass shootings in the United States [Boyd and Molyneux, 2021], and disease spread ([Park et al., 2020], [Unwin et al., 2021]). The use of self-exciting point processes for the modeling of the COVID-19 virus is a natural fit as the model mimics the contagion process in a simple, yet realistic manner. A person becomes infected from a (potentially) unknown source, and they may then spread the virus to others for some period of time, over which the level of contagion gradually decays.

In addition to the initiation of the COVID-19 pandemic, the year 2020 also featured a presidential election in the United States in which the incumbent, President Donald Trump, sought re-election against challenger

Joseph Biden. President Trump held five presidential campaign rallies during the beginning phases of the COVID-19 outbreak, from February 11 to May 20, before temporarily suspending future rallies. After a brief hiatus, the rallies continued, beginning on June 20, 2020 in Tulsa, Oklahoma. These campaign rallies are of interest as they were typically large in size, with participation ranging from hundreds to over 30,000 attendees [Lock, 2020], with little social distancing or mask-wearing by the participants [Rascoe, 2021].

A central question to address is how these rallies impacted the number of people infected with the virus in counties where the rallies took place. Previous researchers have sought to address this question with the use of causal inference modeling [Bernheim et al., 2020], whereby the authors compare the number of infections observed with a counterfactual model which predicts the number of infections that might have occurred had the rallies not taken place.

Some COVID-19 studies (not related to campaign rallies) also rely on the use of the synthetic control method (SCM) to investigate factors impacting the spread of COVID-19, such as school re-openings [Alfano et al., 2021] or local air quality [Cole et al., 2020]. SCM was developed to allow for the evaluation of an intervention by comparing the intervention (treatment) group to a weighted combination of groups that received no treatment as a proxy for a control group [Abadie and Gardeazabal, 2003] and has emerged as an especially pertinent analysis approach for political science and epidemiology studies [Rehkopf and Basu, 2018]. Implementing SCM can be a challenge, however, as the method assumes similarity among treatment and control units, a lack of contamination from the treatment unit into the control units, and a lack of external “shocks” that may impact the control units [Bouttell et al., 2018]. Furthermore, the ability to verify these assumptions requires vast field-specific knowledge of the data, and there exists no consensus on what constitutes a sufficient amount of similarity between treatments and controls.

In this article, we investigate the impact of President Trump’s rallies on COVID-19 outbreaks with the use of a nonparametric variant of the self-exciting point process model. In doing so, we develop statistical methods which can be used in place of traditional causal inference methods without the need to specify synthetic controls. In Section 2, we provide background information on self-exciting point process models and the adaptations to the model we employ to estimate the excess number of cases induced by an event and the duration of the excess. We also describe how the model is estimated and then demonstrate it via simulation in Section 3. The method is then applied in Section 4 by estimating the excess infections, as well as the duration of the excess, from 2020 election campaign rallies. We end with a discussion of the results and our method in Section 5.

2 Modeling and estimation methods

In this section, we start by giving relevant background information about self-exciting point process models. We then describe our adaptations to these models to estimate the excess number of points induced by an event as well as the duration of time in which the excess occurs.

2.1 Self-exciting point processes

Self-exciting point processes, also referred to as Hawkes processes [Hawkes, 1971], model the rate for points, x_i $i = 1, 2, \dots, n$, accumulating in infinitesimally small regions of time

$$\lambda(t|\mathcal{H}_t) = \lim_{\Delta t \rightarrow 0} \frac{E[N([t, t + \Delta t])|\mathcal{H}_t]}{\Delta t}$$

through the use of a counting measure, $N(\cdot)$. The rate at which points occur are typically modeled via their *conditional intensity* functions, $\lambda(\cdot|\mathcal{H}_t)$, where \mathcal{H}_t denotes the the historical occurrence of points from an initial time, t_0 , up to time t , $t > t_0$ [Daley and Vere-Jones, 2004]. For applications of points occurring in time, these conditional intensity functions often take on the form

$$\lambda(t|\mathcal{H}_t) = \mu + \sum_{i:t_i < t} \nu(t - t_i)$$

where μ , here taken to be a positive-valued constant, describes the stochastic occurrence of *background points* (i.e. parent points not directly caused by previous occurrences), and $\nu(t - t_i)$ describes the triggering, or self-exciting, mechanism of the process. The triggering function, $\nu(t - t_i)$, is the component responsible for the *self-exciting* moniker. The function describes how child points are produced, either from background points or subsequent children of the background points. The triggering function further defines how the self-excitation decays over time such that the contagion-like process of a point does not continue indefinitely.

2.2 Model adaptations for estimating effects of outside events

For this article, we utilize a conditional intensity function of the form

$$\lambda_\ell(t|\mathcal{H}_{\ell,t}) = \mu_\ell + K_\ell(t) \sum_{i:t_i < t} g_\ell(t - t_i). \quad (1)$$

Here, $\lambda_\ell(t|\mathcal{H}_{\ell,t})$ describes the conditional intensity for the occurrence of points at time t and location ℓ , $\ell = 1, 2, \dots, m$, given the history of occurrences for location ℓ up to time t , $\mathcal{H}_{\ell,t}$. In the application we describe in Section 4, we model COVID-19 infections for the ℓ^{th} county in which a campaign rally was held for then President, Donald Trump. Thus, m would denote the total number of counties in the United States in which campaign rallies took place. We take μ_ℓ to be the baseline rate of new points occurring in the ℓ^{th} location and $K_\ell(t)$ to be the expected number of subsequent points caused by previous ones, which we refer to as *productivity*. We let $K_\ell(t)$ be a function of time, with additional details given below. The triggering function, $g_\ell(t - t_i)$, describes how the rate of the occurrence of additional points, caused by previous points, decays over time for location ℓ . In this formulation of the conditional intensity function, the parameter μ_ℓ , the parameters of the function $K_\ell(t)$, and the function $g_\ell(t - t_i)$ are considered unknown and must be estimated from the data for location ℓ . Rather than adopt a parametric form, such as exponential or power law decay, to describe how the influence of previous points decays over time, the triggering function, $g_\ell(t - t_i)$, is estimated nonparametrically using histogram estimators which we describe in section 2.3.

Time varying productivities, such as $K_\ell(t)$ used in Equation 1, have been explored to some degree in peer-reviewed literature [Schoenberg et al., 2019] and in pre-print form [Schoenberg, 2020]. The use of time varying productivities with the intent of estimating the additional productivity linked to an external event, to our knowledge, is a novel application; consequently, we describe our further adaptations to the model in Equation 1 here.

Let $K_\ell(t)$ be defined as

$$K_\ell(t) = k_\ell + k_\ell^* \cdot I_{(t_\ell^* < t < t'_\ell)} + k'_\ell \cdot I_{(t'_\ell < t)}$$

where $I_{(\cdot)}$ represents the indicator function. The parameter k_ℓ is taken to be the *baseline* expected number of additional points that are caused by previous ones in location ℓ . The parameter k_ℓ^* describes the additional expected number of points, in addition to the baseline k_ℓ , which are caused by some known outside event taking place at time t_ℓ^* in location ℓ . This additional expected rate of points occurring will last for some unknown duration which ends at time t'_ℓ , $t'_\ell > t_\ell^*$. Finally, k'_ℓ describes the change in the base rate of expected points once the duration of the extra productivity induced by the outside event has diminished. With these modifications in place, we thus adopt the conditional intensity function for location ℓ as

$$\lambda_\ell(t|\mathcal{H}_{\ell,t}) = \mu_\ell + (k_\ell + k_\ell^* \cdot I_{(t_\ell^* < t < t'_\ell)} + k'_\ell \cdot I_{(t'_\ell < t)}) \sum_{i:t_i < t} g_\ell(t - t_i) \quad (2)$$

Using the conditional intensity function as proposed in Equation 2, we estimate constant values for the baseline productivity of previous points, k_ℓ , the additional productivity induced by some outside event occurring at some known time, k_ℓ^* , and how the baseline rate of productivity has changed once the added productivity associated with the outside event has waned, k'_ℓ . We further estimate the end time of the additional productivity, t'_ℓ .

By estimating k_ℓ^* and t'_ℓ , we compute the expected number of points which occurred in excess of the baseline as well as the duration of time, $(t'_\ell - t_\ell^*)$, in which these additional points occurred. This formulation is beneficial as, in instances where the outside event does not add additional productivity over the baseline rate, we would expect the model to produce estimates for k_ℓ^* and $(t'_\ell - t_\ell^*)$ which are close to zero. This expectation then implies that we have a means to identify situations where the outside event did not seem to have an identifiable impact on the rate of points occurring for individual locations.

2.3 Model estimation

To estimate the model parameters and triggering function of Equation 2, we adopt, with several modifications described below, the nonparametric Model Independent Stochastic Declustering (MISD) algorithm proposed by Marsan and Lengliné [Marsan and Lengliné, 2008]. The MISD algorithm, a variant of the EM-algorithm [Dempster et al., 1977], allows for a causal structure for the occurrence of points to be calculated probabilistically using an iterative process to estimate the probability that a point was caused by a previous point, or conversely is a background point. These probabilities are then used to estimate the constant values of

step-functions for the triggering function, referred to as histogram estimators, as well as parameters for the background rate and productivity.

For the histogram estimators, the pairwise differences in times of the events are computed, and then each inter-event time difference is placed into a set of disjoint intervals or bins. Based on the probabilities of the iterative process, constant values are estimated for each interval in order to fit the model. The algorithm utilizes a lower-triangular probability matrix, \mathbf{P} , such that p_{ij} represents the probability that event i is triggered by event j , for $i > j$, while p_{ii} represents the probability that event i is a background point. The algorithm iterates over a sequence of steps in which estimates of the background rate, triggering functions, and probability matrix are updated until convergence has been attained. A more detailed description of the algorithm and standard error estimates may be seen in Fox et al. [2016].

In our approach, $K_\ell(t)$ is a step-function with constants $\{k_\ell, k_\ell^*, k'_\ell\}$ estimated for time-periods $\{(t_{0_\ell}, t_\ell^*], (t_\ell^*, t'_\ell], (t'_\ell, T_\ell]\}$, respectively. Here, t_{0_ℓ} denotes the starting point in which we estimate the *baseline* productivity for location ℓ , t_ℓ^* denotes when the outside event occurs, t'_ℓ denotes when the extra productivity ends that is induced by the event, and T_ℓ denotes the end of the time period. Each value of $K_\ell(t)$ is estimated using the parentage probability matrix with

$$k_\ell = \sum_{j:t_j \in (t_a, t_b]} \sum_{i=j+1}^N \frac{p_{ij}}{(t_b - t_a)}$$

where t_a and t_b denote the beginning and ending times for the time-periods $\{(t_{0_\ell}, t_\ell^*], (t_\ell^*, t'_\ell], (t'_\ell, T_\ell]\}$.

While the starting time for the extra productivity induced by an event, t_ℓ^* is known, the end time of the extra productivity, t'_ℓ , is not and must be estimated. To estimate t'_ℓ , we start by setting $t'_\ell = t_\ell^* + 1$, which can be thought of as the extra productivity lasting only for a single day, and then iterate through each possible length for the duration until $t'_\ell = T_\ell$, computing the value of k'_ℓ for each iteration. We then fit a LOESS curve Cleveland [1979] to the durations of the extra productivity and the estimates of k'_ℓ to determine the day in which the first maximum occurs. Setting t'_ℓ to be the date of the first maximum can be thought of as the date in which the extra productivity begins to wane and the process begins to fall back down to the baseline level of productivity.

To reduce the chance of our procedure erroneously specifying t'_ℓ that is different from t_ℓ^* when the event did not in fact induce any extra productivity, we compare the average number of points occurring just before the event to the average number of points occurring just after the event using a two-sample t-test. In our application, for example, we compared the COVID-19 cases for each county in which then President Trump held a campaign rally and compared the average number of cases which occurred two-weeks before the rally to the average number of cases which occurred two-weeks after. In this example, two-weeks before/after was selected roughly based on the time in which an infected individual remains contagious [Cevik et al., 2021]. If the t-test returns a non-significant p-value, we then state that the event occurring at time t_ℓ^* did not induce any extra productivity.

3 Simulation Study

In order to assess the performance of our modified model and MISD algorithm, we implement a small simulation study. In this study, we are specifically interested in examining how well our proposed method detects the true duration of the increased productivity period as well as its ability to estimate the average increase.

For our study, we simulate points for 100 days in 250 locations using the method for simulating self-exciting point processes described in Zhuang et al. [2004]. We use a background rate of $\mu = 3$ and an exponential temporal decay with rate 0.25 to mimic the rate of decay we roughly observe in our application (Section 4).

For each location, an “event” will take place on the 31st day which will increase the productivity of future points occurring for a duration of 0, 10, 20, 30, or 40 days. After the duration of the extra productivity ends, the productivity returns to a slightly higher than baseline value, which again mimics what we found in our real-data application. For simulated locations in which the duration of the additional productivity is zero, we maintain the baseline level of productivity which enables us to assess our method’s ability to avoid detecting erroneous added productivity when none is present.

The simulation method we employ simulates points in time as positive real numbers, $t_i \in (0, 100]$ and is parameterized using the average number of child-points each individual point is expected to produce. We

aggregate the points occurring in each day to mimic the case-counts data used in our application. In the simulations where the event occurring on day 31 causes a temporary elevation in the occurrence of points, we start with a baseline expected number of offspring points of 0.2 which, once the event occurs, increases to 1.0, a five-fold increase, before falling back down to 0.4 once the effect of the event wanes, a two-fold increase relative to the baseline. For simulations in which no productivity increase occurs, we set the expected number of offspring to be 0.2 for each time period, before and after the event. A summary of the scenarios used in our simulation can be seen in Table 1.

Table 1: Summary of simulation scenario parameters

Number of locations	Duration of extra productivity	Additional productivity
50	0	No increase
50	10	5-fold increase
50	20	5-fold increase
50	30	5-fold increase
50	40	5-fold increase

The results from the simulation study pertaining to the estimation of the duration for increased productivity are outlined in Table 2. For each duration, the minimum, 5th percentile, 25th percentile, median, 75th percentile, 95th percentile, and maximum error in the duration estimates are computed by comparing the estimated duration of the extra productivity to the actual duration, $(\hat{t}'_{\ell} - \hat{t}^*_{\ell}) - (t'_{\ell} - t^*_{\ell})$. Errors which are positive thus correspond to the method over-estimating the duration and vice versa when the estimated duration under-estimates the duration.

Table 2: Differences between estimated and actual durations from simulations

True Duration	Minimum	5th	25th	Median	75th	95th	Maximum
0	0	0	0	0.0	0	9	26
10	-10	-5	-1	1.0	2	3	5
20	-9	-5	-1	1.0	2	3	4
30	-7	-5	0	1.0	2	3	4
40	-4	-2	0	1.5	3	3	3

For instances in which the duration of additional productivity was 0 days, our method incorrectly estimated a duration greater than 0 four times. When the duration was 10 days, we fail to detect the additional productivity once. In the simulation scenarios with non-zero durations, the median error was at most 1.5, with an overwhelming majority of model-produced estimates within a few days of the true durations, yielding an interquartile range of -5 days to +3 days at its largest. Even at the extremes, the model estimates the duration to be within 10 days of the true value which is not entirely unexpected given the variability of self-exciting point processes.

Table 3 shows the estimated additional productivity, k_{ℓ}^* , for each set of 50 simulated locations for each duration in which additional productivity was present. We again present the minimum, maximum, and 5th, 25th, 50th, 75th, 95th percentiles of the estimates. Note as well that, ideally, the estimated additional productivity should be close to five as we employed a five-fold increase in our simulations.

Table 3: Estimated additional productivity relative to baseline from simulations

Durations	Minimum	5th	25th	Median	75th	95th	Maximum
10	0.00	0.83	1.27	1.77	2.37	3.70	23.01
20	0.00	1.35	2.52	3.27	4.47	5.44	18.30
30	0.94	1.28	3.08	4.26	5.21	6.22	6.97
40	0.85	1.59	3.71	5.73	6.58	9.02	10.54

From the table, we see that the median estimated additional productivity starts smaller than the five-fold increase we expected, for the 10-day duration simulations, and gradually increases as the duration increases.

For the 40-day duration catalogs, the productivity increase is very near what is expected with the middle 50% of the estimates ranging from 3.71 to 6.58. Given that it takes some amount of time for the additional productivity to fully develop in the simulations, we do not view the estimates for the 10-day and 20-day durations as inaccurate. Rather, we view them as being plausible estimates for the true amount of additional productivity that could be realized over relatively short time-spans. Additionally, we note that as the duration of the extra-productivity time-period increases, the point process has a larger time span in which to generate points, making the longer time-durations better at estimating the five-fold increases used when generating the data. We also notice that, as the duration increases, the 95th percentile also grows which, again, is not unexpected given the inherent variability of self-exciting point processes.

Overall, we find the ability of our proposed method to estimate the duration and additional productivity of the simulated catalogs to be rather strong, though we note that it is also capable of producing inaccurate estimates on occasion. It is entirely plausible that altering certain parameters of the modified MISD algorithm, such as changing the LOESS smoothing bandwidth or the time intervals in which we estimate the decay of the points, may have improved the estimates further. However, we avoid doing this so as not to overfit the simulated catalogs of points.

4 Application: Estimating excess infections and their durations for 2020 election campaign rallies

In this section, we apply our modified self-exciting point process model, described in Section 2, to daily COVID-19 case counts data for each county in which then President Donald Trump held a campaign rally during the 2020 United States election cycle. We start with a description of the data used in our analysis in Section 4.1 and then describe our evaluation methods and results in Section 4.2 and Section 4.3, respectively.

4.1 Data

COVID-19 data for this project was taken from the *New York Times* [2021], reporting daily case counts in the United States at the county level. Recorded COVID-19 cases in the United States began on January 21, 2020 in Snohomish County, Washington, with subsequent case counts being maintained daily. As county level reporting is the finest resolution available, we use this data to track COVID-19 cases within the counties, rather than cities, in which then President Trump held a campaign rally during his 2020 re-election campaign. For each county, data was drawn 30 days prior to the campaign rally in order to estimate the baseline productivity of viral transmission. We then used data, for each county, occurring 150 days after the rally was held to provide sufficient time to encapsulate the duration of any additional productivity induced by the campaign rally.

In this application, we study the effects of rallies held during the COVID-19 pandemic, beginning on June 20, 2020 and concluding on November 2, 2020. In total, 67 rallies were held on or after June 20; of these 67 rallies, 65 rallies were held in cities/towns that fall within designated counties. President Trump held repeat rallies in three counties (Cumberland, North Carolina; Lackawanna, Pennsylvania; Maricopa, Arizona). For these three counties, only the first rally held in each location will be considered as the during-rally effect of the first rally may still be present at the time of the second rally. Focusing on only the initial rally will also prevent the double counting of potentially rally-related cases. After removing repeated rally counties and non-county affiliated rallies, the remaining 62 rallies will be used in this study and are highlighted in Figure 1.

Though official attendance numbers are not publicly available for any rally, rough estimates have been reported by local news organizations. Such estimates were obtained for each rally in order to verify that attendance was large enough to potentially spur additional cases within the county. A few smaller rallies hosted hundreds of attendees, while most rallies were attended by thousands of individuals. The self-exciting point process models introduced in Section 2 and further specified in Section 4.2 below do not require attendance data, so the lack of precise records will not impede analyses.

4.2 Evaluation methods

To verify whether an increase in cases at the county level may be attributed to President Trump’s campaign rallies, or was simply part of a broader trend within the state, we will compare the increase of cases seen within a rally county to the increase in cases within the state as a whole. After applying the MISD algorithm to the county in which a campaign rally took place, we then use the same modeling approach to the respective state while specifying the same the pre-, during-, and post-rally time-periods estimated by the county level

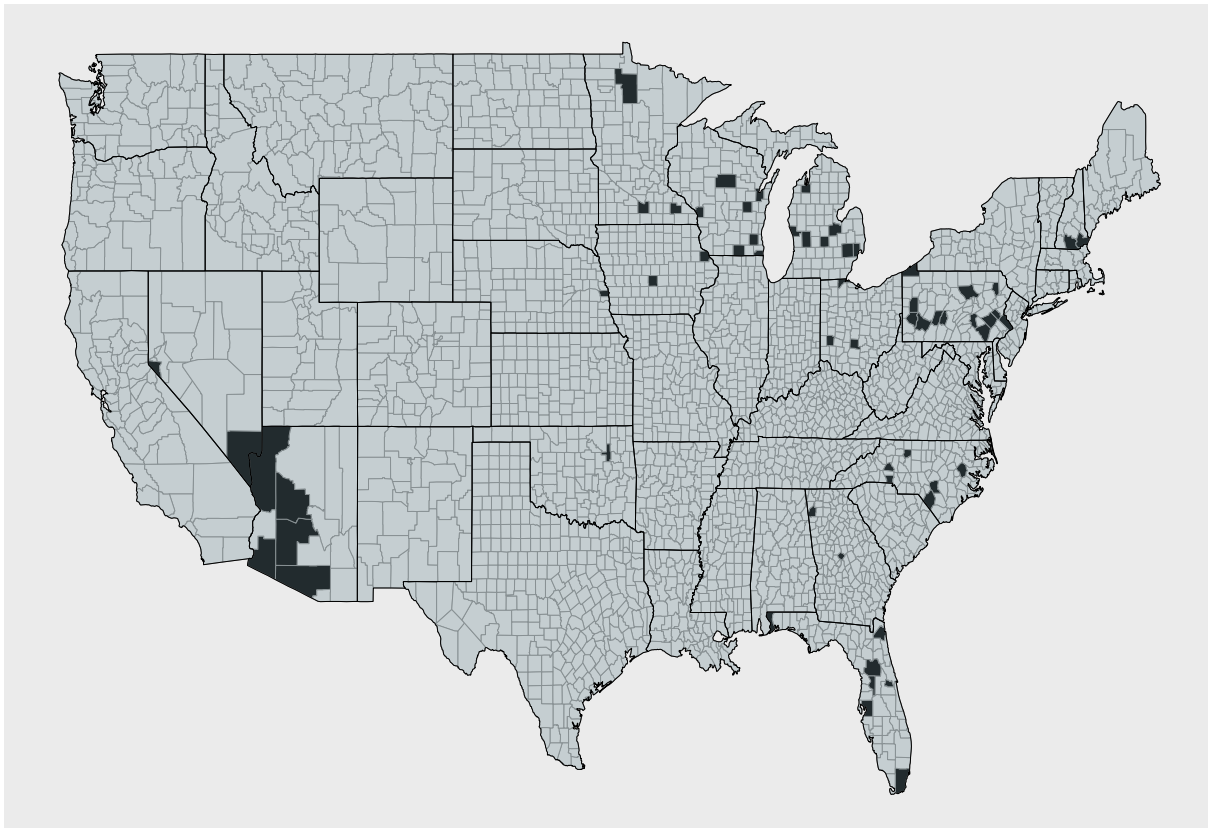


Figure 1: Counties within the United States that hosted a President Trump campaign rally in 2020.

model. To focus more directly on the pattern of COVID cases happening in the state and limit interaction with rallies, the statewide model includes case data from only counties in which President Trump did not hold a rally at any point.

Once the county and state models have been fit, we estimate the number of cases that may be linked to President Trump’s campaign rallies in the following manner. We first find the population adjusted increase in productivity at both the county and state levels for location ℓ and produce the multiplier, κ_ℓ , such that

$$\kappa_\ell = \frac{k_{\ell_{\text{county}}}^* - k_{\ell_{\text{county}}}}{\text{population}_{\ell_{\text{county}}}} - \frac{k_{\ell_{\text{state}}}^* - k_{\ell_{\text{state}}}}{\text{population}_{\ell_{\text{state}}}},$$

where the subscripts “county” and “state” denote county and state level estimates for location ℓ , respectively. We may then find the estimated number of cases resulting from a rally, above what was observed in the rest of the state, via

$$\text{cases}_\ell = \kappa_\ell \times \text{population}_{\ell_{\text{county}}} \times (t'_\ell - t_\ell^*) \quad (3)$$

where $(t'_\ell - t_\ell^*)$ defines the duration (in days) in which the rally county experiences a heightened productivity.

4.3 Application results

Table 4 displays the 34 campaign rallies that were found to have a significant increase of COVID-19 cases following a campaign rally, which we refer to as a *rally effect*, relative to the rest of the state. The table includes the county and state in which the rally was held and the date the rally took place. It reports the estimated background rate of infection (μ_ℓ), the baseline productivity of additional infections before the rally took place (k_ℓ), the estimated additional productivity of infections linked to the campaign rally (k_ℓ^*), and the

estimated number of days the rally effect persisted as well as the estimated number of cases resulting from the rally based on Equation 3.

Table 4: Counties in which an increase in COVID-19 productivity, over baseline, was found following campaign rallies held by then President Donald Trump during the 2020 United States election cycle

County	State	Date of Rally	μ_ℓ	k_ℓ	k_ℓ^*	Duration	Cases
Tulsa	OK	2020-06-20	57.43	0.00	183.40	50	4274
Blue Earth	MN	2020-08-17	7.01	6.25	17.07	22	315
Marathon	WI	2020-09-17	6.69	0.12	159.75	61	8602
Beltrami	MN	2020-09-18	1.53	0.79	29.40	87	1362
St. Louis	MN	2020-09-30	4.81	35.20	148.57	59	4334
Cambria	PA	2020-10-13	4.82	1.04	124.57	64	5353
Polk	IA	2020-10-14	34.09	58.81	431.27	40	10676
Muskegon	MI	2020-10-17	4.66	6.86	190.78	31	4690
Rock	WI	2020-10-17	6.99	51.27	174.50	29	2743
Yavapai	AZ	2020-10-19	7.88	5.81	148.44	75	3603
Pima	AZ	2020-10-19	38.44	24.15	818.36	95	25203
Erie	PA	2020-10-20	10.69	0.09	154.64	69	3334
Escambia	FL	2020-10-23	10.26	16.70	269.84	96	4023
Pickaway	OH	2020-10-24	2.89	13.09	50.20	79	834
Waukesha	WI	2020-10-24	11.92	161.38	883.63	30	18765
Hillsborough	NH	2020-10-25	24.82	0.49	254.46	88	5159
Lehigh	PA	2020-10-26	23.22	0.17	262.07	81	7509
Lancaster	PA	2020-10-26	37.49	12.67	291.96	65	3905
Blair	PA	2020-10-26	3.57	14.19	122.92	53	3527
Clinton	MI	2020-10-27	10.66	3.79	101.86	20	1627
La Crosse	WI	2020-10-27	5.59	41.96	146.63	16	1346
Douglas	NE	2020-10-27	25.29	203.08	787.79	25	11056
Mohave	AZ	2020-10-28	6.75	0.06	182.05	81	6510
Oakland	MI	2020-10-30	124.66	73.24	1257.86	17	15342
Olmsted	MN	2020-10-30	7.55	23.08	169.99	22	2313
Bucks	PA	2020-10-31	47.23	0.19	355.42	52	6205
Berks	PA	2020-10-31	50.76	37.22	274.95	77	3242
Butler	PA	2020-10-31	15.57	5.36	147.12	57	3773
Lycoming	PA	2020-10-31	6.57	0.83	94.47	59	2872
Macomb	MI	2020-11-01	141.74	75.83	1059.51	13	10301
Catawba	NC	2020-11-01	7.35	45.56	132.87	82	1052
Miami-Dade	FL	2020-11-01	351.71	165.67	2312.79	75	67006
Grand Traverse	MI	2020-11-02	6.93	10.29	57.94	29	570
Kenosha	WI	2020-11-02	5.03	74.82	204.56	20	1629

Table 5 shows the minimum, maximum, and the 5th, 25th, 50th, 75th, 95th percentiles of the estimated additional productivity relative to the baseline, the duration of the effect, and the additional number of cases relative to the rest of the state for the counties in which contained a rally-effect.

For counties in which a rally effect was detected, there was a 6-fold increase in the median productivity of COVID-19 cases with an inter-quartile range of 7.72. The median duration of this increase was roughly two months with a minimum duration of about two weeks and a maximum increase of about three months. Additional cases, which we attribute to the rally after taking into account the changes seen at the state level, ranged from a few hundred up to tens of thousands with a median estimate of about 4000 additional cases per rally.

The 28 counties in which campaign rallies were estimated to have little to no impact by our model, or were estimated to have little to no impact relative to the rest of the state, are shown in Table 6. The table also includes counties for which the model estimation processes failed to converge, which is a known issue for

Table 5: Estimated additional productivity relative to baseline from simulations

	Minimum	5th	25th	Median	75th	95th	Maximum
Additional productivity relative to baseline	1.29	2.54	3.39	6.09	11.11	22.03	26.73
Duration	13.00	16.65	29.00	58.00	76.50	90.45	96.00
Additional cases	315.00	741.60	2420.50	3964.00	7259.25	21018.30	67006.00

self-exciting processes [Veen and Schoenberg, 2008]. The information contained in the table is similar to that of Table 4 except for the additional column which describes whether the model estimation process failed to converge.

Table 6: Counties in which little to no increase in COVID-19 productivity, over baseline, was found following campaign rallies held by then President Donald Trump during the 2020 United States election cycle

County	State	Date of Rally	μ_ℓ	k_ℓ	k_ℓ^*	Duration	Cases	Converged?
Maricopa	AZ	2020-06-23	-	-	-	-	-	No
Winnebago	WI	2020-08-17	15.23	0.03	0	0	0	Yes
Yuma	AZ	2020-08-18	-	-	-	-	-	No
Lackawanna	PA	2020-08-20	17.29	0	0	0	0	Yes
Rockingham	NH	2020-08-28	26.89	0	0	0	0	Yes
Westmoreland	PA	2020-09-03	12.61	0	0	0	0	Yes
Forsyth	NC	2020-09-08	52.05	0.07	0	0	0	Yes
Saginaw	MI	2020-09-10	23.48	0.03	0	0	0	Yes
Douglas	NV	2020-09-12	3.06	0	0	0	0	Yes
Clark	NV	2020-09-13	252.04	131.97	0	0	0	Yes
Cumberland	NC	2020-09-19	42.79	13.57	0	0	0	Yes
Montgomery	OH	2020-09-21	36.32	64.87	0	0	0	Yes
Lucas	OH	2020-09-21	34.61	0.57	0	0	0	Yes
Allegheny	PA	2020-09-22	65.1	0.16	0	0	0	Yes
Duval	FL	2020-09-24	99.78	49.46	0	0	0	Yes
Dauphin	PA	2020-09-26	10.25	8.87	113.52	115	0	Yes
Seminole	FL	2020-10-12	30.51	0.07	147.76	106	0	Yes
Pitt	NC	2020-10-15	11.78	37.65	0	0	0	Yes
Marion	FL	2020-10-16	23.49	13.7	0	0	0	Yes
Bibb	GA	2020-10-16	9.44	13.99	0	0	0	Yes
Gaston	NC	2020-10-21	15.74	64.38	0	0	0	Yes
Sumter	FL	2020-10-23	6.85	20.41	0	0	0	Yes
Robeson	NC	2020-10-24	6.63	49.83	0	0	0	Yes
Hillsborough	FL	2020-10-29	109.55	107.71	631.31	84	0	Yes
Brown	WI	2020-10-30	14.68	432.95	0	0	0	Yes
Dubuque	IA	2020-11-01	3.85	121.99	0	0	0	Yes
Floyd	GA	2020-11-01	8.26	36.13	42.04	10	0	Yes
Kent	MI	2020-11-02	-	-	-	-	-	No

In Table 6, we see that there were three instances when the estimation method failed to converge, specifically for Maricopa County, Arizona, Yuma County, Arizona, and Kent County, Michigan. These failures were due to some volatility in the case counts occurring in the 30 days prior to the campaign rally as we were able to get the models to converge when using data from 32 to 35 days prior to the rally. To keep our comparisons similar, we omit the estimates based on these lengthend before-rally time periods. We further note that there were 22 instances where the model detected no rally-effect and four instances in which the estimated

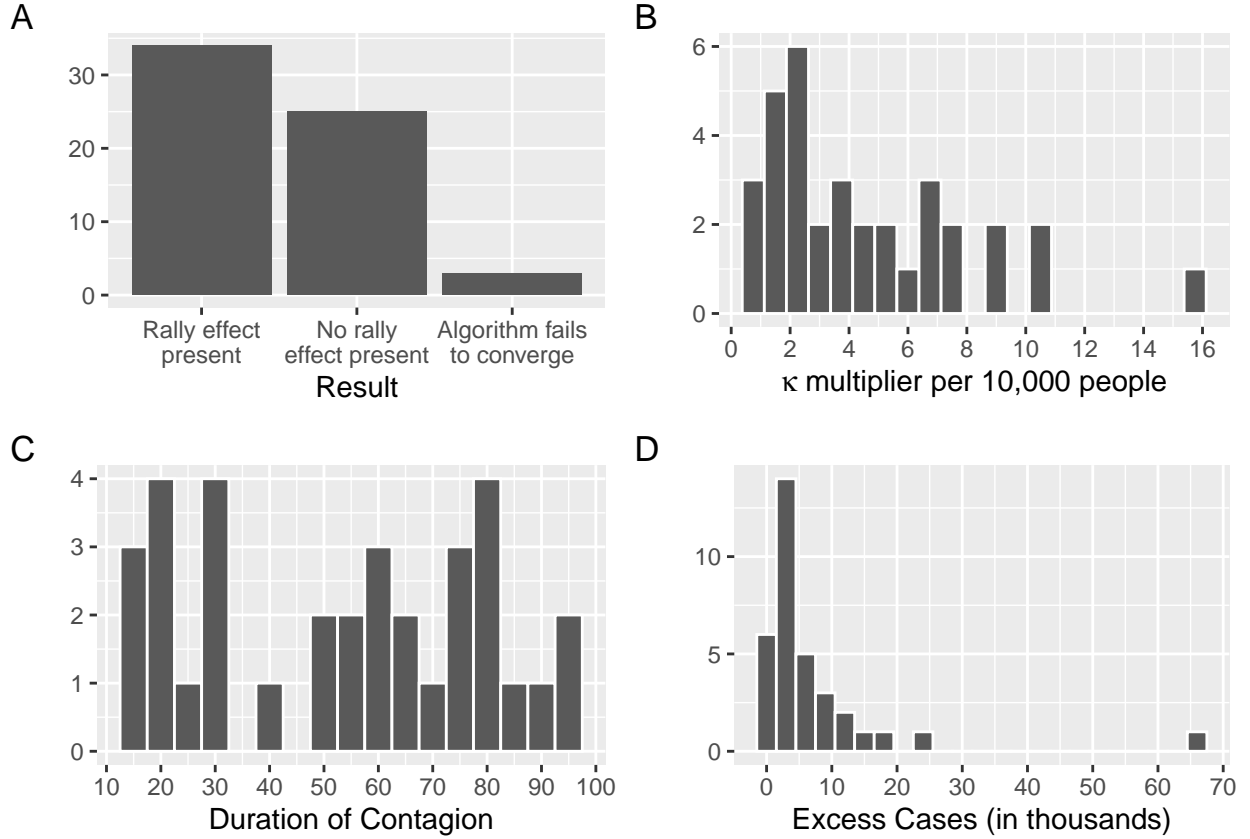


Figure 2: (A) Distribution of county level results in which the rally may have contributed to an increase in cases beyond the state level, had no impact on cases, increased cases but at a rate lower than state increases, or the algorithm failed to converge. (B) Distribution of the multiplier seen in Equation 3. (C) Distribution of the duration in which the additional contagion is estimated to last following the rally. (D) Distribution of the number of excess cases that may be attributed to President Trump’s rallies.

rally-effect was not distinguishable compared to the case counts from the rest of the state containing the county.

Figure 2 provides distributions of several results, namely the number of cases, the κ multiplier seen in Equation 3, the duration of the excess contagion, and the overall assessment of the rally on COVID-19 cases. Figure 3 then shows the results of the model estimation over the time in which campaign rallies took place.

In Figure 3, we note that between August and October, the majority of the campaign rallies were estimated to have no impact on the daily COVID-19 case numbers or were estimated to be no different than what was observed at the state level. Counties in which a rally effect was found during these months tended to have populations which were approximately five-times smaller, on average, than counties where no effects were present (mean populations of 110,000 vs. 550,000, respectively). We postulate that, given the state of the epidemic during those months, the model was more adept at detecting additional productivity in these smaller counties than in counties with larger populations.

5 Discussion

In this article, we adapt temporal self-exciting point process models and their nonparametric estimation techniques to estimate the duration and effects that events, occurring at some time and place, have on the productivity of the occurrence of subsequent points. In doing so, we develop an alternative modeling approach to the synthetic control methods which are commonly employed to estimate such effects. In our approach,

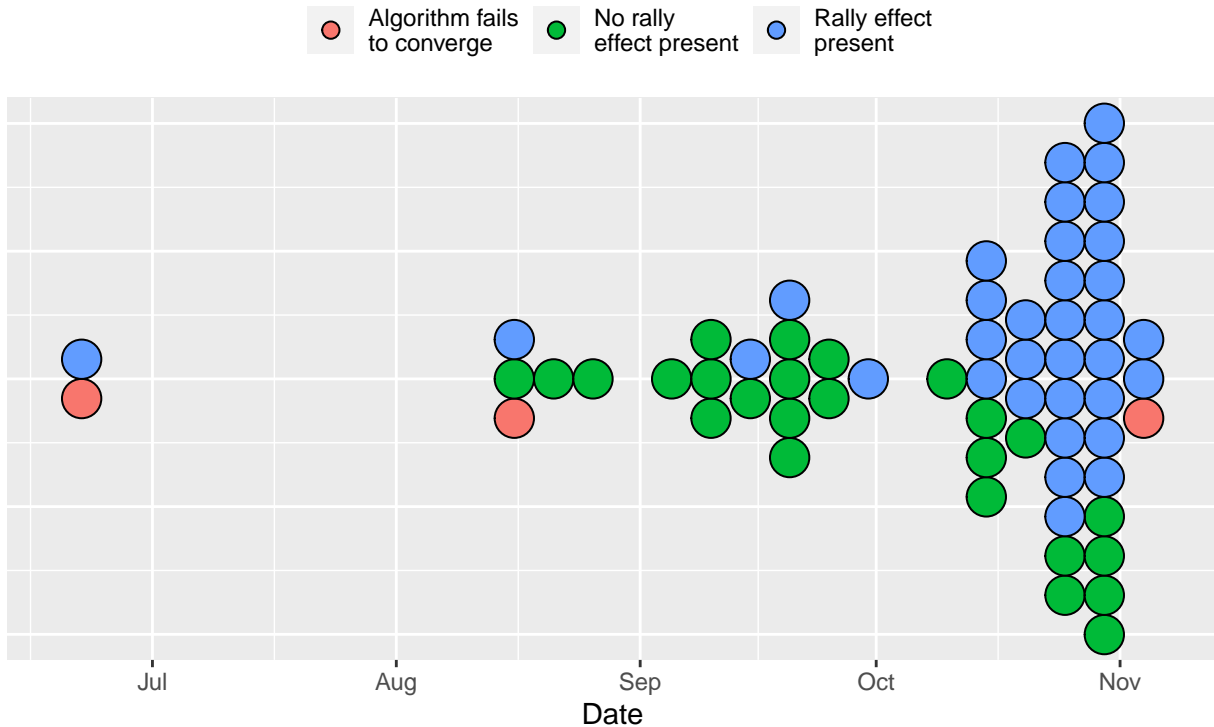


Figure 3: Model estimation outcomes by date of rally. Please note that rallies are binned into 5-day intervals for plotting purposes.

however, we avoid the necessity of finding suitable controls and instead estimate the effects and duration using the data from the location of interest directly.

We apply our methods to study the impact that campaign rallies held by then President Donald Trump had on COVID-19 cases in counties across the United States. By treating daily COVID-19 case counts as a self-exciting point process, we are able to model the change in contagion productivity, if any, which occurred after the rallies. And by fitting models at both the county and state level, we may then estimate the relative number of COVID-19 cases that may be linked to the rally.

In making comparisons between counties in which rallies were held and the states containing the counties, we assume that similar state level pandemic policies would apply uniformly throughout the state; however, we recognize that regulations, political, and social adherence to such policies vary widely across an individual state’s counties [Brzezinski et al., 2021].

While our application demonstrates the method’s ability to detect increases in the occurrence of points, or COVID-19 cases, the approach would be equally well-suited for applications in which a reduction in the occurrence of points is thought to occur. Our methods are also relatively simple compared to regression modeling techniques, needing only the daily case counts to fit the model.

Similar to the findings of Bernheim et al. [2020], and in contrast to the findings of Dave et al. [2021], we find that the campaign rally which took place in Tulsa, Oklahoma on June 20, 2020, did lead to an increase in COVID-19 cases for that county. Further, Bernheim et al. [2020], who used synthetic control methods to estimate the campaign rally-related increase in COVID-19 infections for 18 rallies held between June 20, 2020 and September 30, 2020, estimated the overall number of rally related cases to be approximately 30,000 additional infections. This leads to an estimated increase of approximately 1600 additional cases per rally. Using our proposed methods, we find that, on average in the counties for which an increase in infection productivity was detected, there was approximately 750 additional cases per rally. Our method, however, compares the estimated increase in case counts within the counties to their respective states, rather than to the synthetic controls. We also estimate the duration of the additional productivity rather than comparing infection rates for a 10-week period following the rally.

Overall, we estimate the total number of COVID-19 cases that may be attributed to the 62 campaign rallies used in our study to be 253,055. We further observe that 34 of 62 rallies were estimated to yield an excess of COVID-19 cases while 25 rallies showed no evidence of increase in case numbers.

References

- Alberto Abadie and Javier Gardeazabal. The economic costs of conflict: A case study of the basque country. *American Economic Review*, 93(1):113–132, March 2003. doi: 10.1257/000282803321455188. URL <https://www.aeaweb.org/articles?id=10.1257/000282803321455188>.
- Vincenzo Alfano, Salvatore Ercolano, and Lorenzo Cicatiello. School openings and the covid-19 outbreak in italy: a provincial-level analysis using the synthetic control method. *Health Policy*, 125(9):1200–1207, 2021. ISSN 0168-8510. doi: <https://doi.org/10.1016/j.healthpol.2021.06.010>. URL <https://www.sciencedirect.com/science/article/pii/S0168851021001676>.
- Earvin Balderama, Frederic Paik Schoenberg, Erin Murray, and Philip W. Rundel. Application of branching models in the study of invasive species. *Journal of the American Statistical Association*, 107(498):467–476, 2012. ISSN 01621459. URL <http://www.jstor.org/stable/23239584>.
- B. Douglas Bernheim, Nina buchmann, Zach Freitas-Groff, and Sebastián Otero. The effects of large group meetings on the spread of covid-19: The case of trump rallies. 2020. URL <https://ssrn.com/abstract=3722299>.
- Andrea L. Bertozzi, Elisa Franco, George Mohler, Martin B. Short, and Daniel Sledge. The challenges of modeling and forecasting the spread of covid-19. *Proceedings of the National Academy of Sciences*, 117(29):16732–16738, 2020. ISSN 0027-8424. doi: 10.1073/pnas.2006520117. URL <https://www.pnas.org/content/117/29/16732>.
- Giorgia Bonalumi, Michele di Mauro, Andrea Garatti, Fabio Barili, Gino Gerosa, Alessandro Parolari, and for the Italian Society for Cardiac Surgery Task Force on COVID-19 Pandemic. The covid-19 outbreak and its impact on hospitals in italy: the model of cardiac surgery. *European Journal of Cardio-Thoracic Surgery*, 57(6):1025–1028, 04 2020. ISSN 1010-7940. doi: 10.1093/ejcts/ezaa151. URL <https://doi.org/10.1093/ejcts/ezaa151>.
- Janet Bouttell, Peter Craig, James Lewsey, Mark Robinson, and Frank Popham. Synthetic control methodology as a tool for evaluating population-level health interventions. *Journal of Epidemiology & Community Health*, 72(8):673–678, 2018. ISSN 0143-005X. doi: 10.1136/jech-2017-210106. URL <https://jech.bmj.com/content/72/8/673>.
- Peter Boyd and James Molyneux. Assessing the contagiousness of mass shootings with nonparametric hawkes processes. *PLOS ONE*, 16(3):1–18, 03 2021. doi: 10.1371/journal.pone.0248437. URL <https://doi.org/10.1371/journal.pone.0248437>.
- Raiha Browning, Deborah Sulem, Kerrie Mengersen, Vincent Rivoirard, and Judith Rousseau. Simple discrete-time self-exciting models can describe complex dynamic processes: A case study of covid-19. *PLOS ONE*, 16(4):1–28, 04 2021. doi: 10.1371/journal.pone.0250015. URL <https://doi.org/10.1371/journal.pone.0250015>.
- Adam Brzezinski, Valentin Kecht, David Van Dijke, and Austin L Wright. Science skepticism reduced compliance with covid-19 shelter-in-place policies in the united states. *Nature Human Behaviour*, 5(11):1519–1527, 2021.
- M Cevik, M Tate, O Lloyd, AE Maraolo, J Schafers, and A Ho. Sars-cov-2, sars-cov, and mers-cov viral load dynamics, duration of viral shedding, and infectiousness: a systematic review and meta-analysis. *The Lancet. Microbe*, Jan 2021. URL <https://pubmed.ncbi.nlm.nih.gov/33521734/>.
- Sang-Wook (Stanley) Cho. Quantifying the impact of nonpharmaceutical interventions during the COVID-19 outbreak: The case of Sweden. *The Econometrics Journal*, 23(3):323–344, 08 2020. ISSN 1368-4221. doi: 10.1093/ectj/utaa025. URL <https://doi.org/10.1093/ectj/utaa025>.
- William S. Cleveland. Robust locally weighted regression and smoothing scatterplots. *Journal of the American Statistical Association*, 74(368):829–836, 1979. doi: 10.1080/01621459.1979.10481038. URL <https://www.tandfonline.com/doi/abs/10.1080/01621459.1979.10481038>.
- Matthew A. Cole, Ceren Ozgen, and Eric Strobl. Air Pollution Exposure and Covid-19 in Dutch Municipalities. *Environmental & Resource Economics*, 76(4):581–610, August 2020. doi: 10.1007/s10640-020-00491-.
- Daryl J Daley and David Vere-Jones. *An Introduction to the Theory of Point Processes Volume I: Elementary Theory and Methods*. Springer Science and Business Media, 2004.

- Dhaval Dave, Drew McNichols, and Joseph J. Sabia. The contagion externality of a superspreading event: The sturgis motorcycle rally and covid-19. *Southern Economic Journal*, 87(3):769–807, 2021. doi: <https://doi.org/10.1002/soej.12475>. URL <https://onlinelibrary.wiley.com/doi/abs/10.1002/soej.12475>.
- A. P. Dempster, N. M. Laird, and D. B. Rubin. Maximum likelihood from incomplete data via the em algorithm. *Journal of the Royal Statistical Society. Series B (Methodological)*, 39(1):1–38, 1977. ISSN 00359246. URL <http://www.jstor.org/stable/2984875>.
- Eric Warren Fox, Frederic Paik Schoenberg, and Joshua Seth Gordon. Spatially inhomogeneous background rate estimators and uncertainty quantification for nonparametric hawkes point process models of earthquake occurrences. *Ann. Appl. Stat.*, 10(3):1725–1756, 09 2016. doi: 10.1214/16-AOAS957. URL <https://doi.org/10.1214/16-AOAS957>.
- Ali Hadianfar, Razieh Yousefi, Milad Delavary, Vahid Fakoor, Mohammad Taghi Shakeri, and Martin Lavallière. Effects of government policies and the nowruz holidays on confirmed covid-19 cases in iran: An intervention time series analysis. *PLOS ONE*, 16(8):1–11, 08 2021. doi: 10.1371/journal.pone.0256516. URL <https://doi.org/10.1371/journal.pone.0256516>.
- Alan G Hawkes. Spectra of some self-exciting and mutually exciting point processes. *Biometrika*, 58(1):83–90, 1971.
- Samantha Lock. Georgia trump rally attendees stranded waiting for buses in campaign chaos, Nov 2020. URL <https://www.newsweek.com/georgia-trump-rally-attendees-stranded-waiting-buses-another-campaign-event-ends-chaos-1543900>.
- Giovanni S P Malloy, Lisa Puglisi, Margaret L Brandeau, Tyler D Harvey, and Emily A Wang. Effectiveness of interventions to reduce covid-19 transmission in a large urban jail: a model-based analysis. *BMJ Open*, 11(2), 2021. ISSN 2044-6055. doi: 10.1136/bmjopen-2020-042898. URL <https://bmjopen.bmj.com/content/11/2/e042898>.
- David Marsan and Olivier Lengliné. Extending earthquakes’ reach through cascading. *Science*, 319(5866):1076–1079, 2008. ISSN 0036-8075. doi: 10.1126/science.1148783. URL <https://science.sciencemag.org/content/319/5866/1076>.
- Yosihiko Ogata. Statistical models for earthquake occurrences and residual analysis for point processes. *Journal of the American Statistical association*, 83(401):9–27, 1988.
- Yosihiko Ogata. Space-time point-process models for earthquake occurrences. *Annals of the Institute of Statistical Mathematics*, 50(2):379–402, 1998.
- Junhyung Park, Adam W. Chaffee, Ryan J. Harrigan, and Frederic Paik Schoenberg. A non-parametric hawkes model of the spread of ebola in west africa. *Journal of Applied Statistics*, 0(0):1–17, 2020. doi: 10.1080/02664763.2020.1825646. URL <https://doi.org/10.1080/02664763.2020.1825646>.
- Roger D Peng, Frederic Paik Schoenberg, and James A Woods. A space-time conditional intensity model for evaluating a wildfire hazard index. *Journal of the American Statistical Association*, 100(469):26–35, 2005. doi: 10.1198/016214504000001763. URL <https://doi.org/10.1198/016214504000001763>.
- Ayesha Rascoe. Trump hits the trail with florida rally, a week after covid-19 hospital stay. *NPR*, October 2021. URL <https://www.npr.org/2020/10/12/923050101/trump-hits-the-trail-with-florida-rally-a-week-after-covid-19-hospital-stay>.
- David H. Rehkopf and Sanjay Basu. A new tool for case studies in epidemiology-the synthetic control method. *Epidemiology*, 2018.
- Frederic Paik Schoenberg. Nonparametric estimation of variable productivity hawkes processes, 2020.
- Frederic Paik Schoenberg, Marc Hoffmann, and Ryan J. Harrigan. A recursive point process model for infectious diseases. *Annals of the Institute of Statistical Mathematics*, 71(5):1271–1287, 2019. doi: 10.1007/s10463-018-0690-9. URL <https://doi.org/10.1007/s10463-018-0690-9>.
- H. Juliette T. Unwin, Isobel Routledge, Seth Flaxman, Marian-Andrei Rizoiiu, Shengjie Lai, Justin Cohen, Daniel J. Weiss, Swapnil Mishra, and Samir Bhatt. Using hawkes processes to model imported and local malaria cases in near-elimination settings. *PLOS Computational Biology*, 17(4):1–18, 04 2021. doi: 10.1371/journal.pcbi.1008830. URL <https://doi.org/10.1371/journal.pcbi.1008830>.
- Alejandro Veen and Frederic P Schoenberg. Estimation of space-time branching process models in seismology using an em-type algorithm. *Journal of the American Statistical Association*, 103(482):614–624, 2008. doi: 10.1198/016214508000000148. URL <https://doi.org/10.1198/016214508000000148>.

Yan Wang. Government policies, national culture and social distancing during the first wave of the covid-19 pandemic: International evidence. *Safety Science*, 135:105138, 2021. ISSN 0925-7535. doi: <https://doi.org/10.1016/j.ssci.2020.105138>. URL <https://www.sciencedirect.com/science/article/pii/S092575352030535X>.

Jiancang Zhuang, Yosihiko Ogata, and David Vere-Jones. Analyzing earthquake clustering features by using stochastic reconstruction. *Journal of Geophysical Research: Solid Earth*, 109(B5), 2004. doi: <https://doi.org/10.1029/2003JB002879>. URL <https://agupubs.onlinelibrary.wiley.com/doi/abs/10.1029/2003JB002879>.